The Journal of Engineering

The 9th International Conference on Power Electronics, Machines and Drives (PEMD 2018)

IET Journals
The Institution of Engineering and Technology

Fluid flow and heat transfer analysis of TEFC machine end regions using more realistic end-winding geometry

eISSN 2051-3305
Received on 21st June 2018
Accepted on 27th July 2018
E-First on 15th April 2019
doi: 10.1049/joe.2018.8026
www.ietdl.org

Salvatore La Rocca[1] ✉, Stephen J. Pickering[2], Carol N. Eastwick[1], Chris Gerada[3], Kristian Rönnberg[4]

[1]*Faculty of Engineering, Fluids and Thermal Engineering Research Group, University of Nottingham, NG7 2RD, UK*
[2]*Faculty of Engineering, Composites Research Group, University of Nottingham, NG7 2RD, UK*
[3]*Faculty of Engineering, Power Electronics, Machines and Control Research Group, University of Nottingham, NG7 2RD, UK*
[4]*ABB AB Corporate Research, Forskargränd 7, 72178 Västerås, Sweden*
✉ *E-mail: salvatore.larocca@nottingham.ac.uk*

Abstract: Here, a typical small low-voltage totally enclosed fan-cooled (TEFC) motor (output power ∼10 kW) has been studied using computational fluid dynamics. The complexity of the end-winding geometries, often consisting of several insulated copper strands bound together, provides a challenge to the modelling and analysis of heat transfer and fluid flow phenomena occurring in the end region, which typically is an area of most interest for thermal management. Approximated geometries are usually employed in order to model the end windings to reduce the analysis time and cost. This paper presents a comparison of two cases, a typical simplified geometry and a more realistic geometry of end windings, and uses these cases to highlight the challenges and impact on predicted heat transfer. A comparison of the two models indicate that the different representations of end winding geometries can affect the heat dissipation rate through the outer housing by up to 45%.

1 Introduction

For electrical machines along with the electromagnetic design, in the last decade thermal design has begun to attract serious attention of design engineers; this can be explained by the fact that the temperature is the main factor in determining capacity for increased specific power density. Industry demands and material costs have seen a continuous rise in required specific power density with machines becoming more compact; this has resulted in higher temperature gradients which can significantly reduce overall efficiency. In addition, temperature impacts the lifetime of the materials, in particular of the insulating materials; for instance, above the maximum temperature allowed for the given insulation class, a rise of 10 K can reduce the lifetime of the insulation by as much as 50% [1].

In the past, motor designers have dealt with the thermal design aspect mostly based on prior knowledge of parameters related to the operating conditions such as winding to ambient thermal resistance or housing heat transfer coefficient [2]. In reality, very complex thermal phenomena involving conduction, convection, and radiation take place in electrical machines and critical thermal modelling is required for investigating the machines thermal behaviour.

Effective thermal management leads to a reduction in winding's temperature-dependent losses and improved airflow can reduce windage losses and thus increases the performance of the machine; with consequential, economic advantages. Totally enclosed fan-cooled (TEFC) rotating electrical machines provide a challenge as the internal flows and heat transfer must be analysed jointly with the external forced flow. Here, a typical small low-voltage TEFC motor (induction motor, 4 poles, 3 phase, output power ∼10 kW) has been studied; Fig. 1 shows the structure of the motor under investigation.

A TEFC induction motor does not permit outside air to freely circulate through the interior of the motor meaning the internal parts are totally isolated from the surrounding air. As of this, TEFC motors can be used in dirty, moist, or mildly corrosive operating conditions [3]. The TEFC motor is cooled by blowing air over the motor frame using an external fan mounted on the rear shaft of the motor. Externally, radial fins running in the axial direction are included on the frame surface in order to increase surface area and, therefore, the convective heat transfer between the frame and surrounding environment [4]. Internally, rotor bar extensions and wafters fixed to the rotor end ring may be used to provide internal stirring and improve the convective heat transfer in the end region area [5].

As the heat removal is dependent on both the internal and external features, this provides a significant challenge as the internal and external flows and heat transfer must be analysed jointly, creating a complex scenario with multiple dependencies. However due to this complexity, some geometric features/areas are commonly simplified and the question is how much this impacts the fidelity of the answer.

The most common techniques used to perform thermal analyses are lumped parameters thermal network (LPTN), computational fluid dynamics (CFD), and finite elements analysis (FEA) [6]. While LPTN provides a very quick answer, it is reliant on accurate estimates of heat transfer coefficients, meaning that its accuracy is limited to known designs [6]. FEA provides a potential route for an accurate calculation of conduction heat transfer in complex geometric shapes; however, its most important limitation is the use

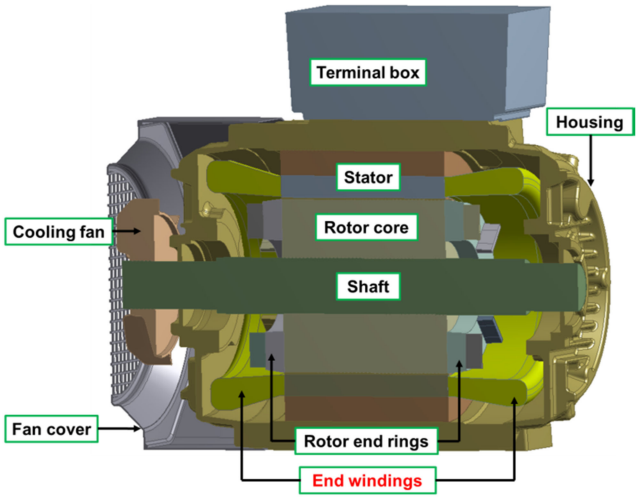

Fig. 1 *TEFC motor structure*

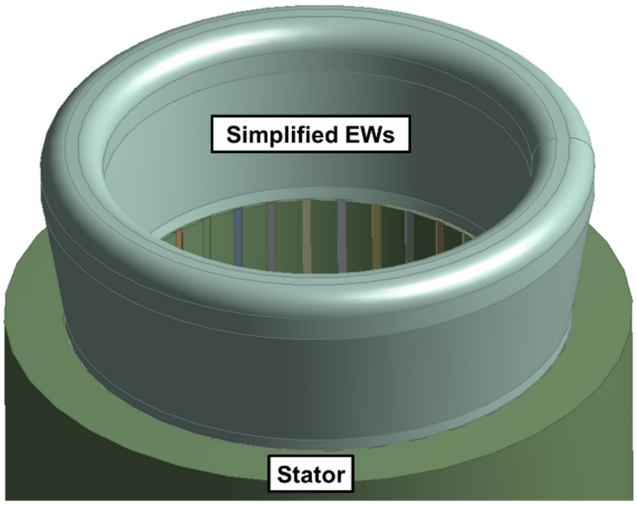

Fig. 2 *Simplified end winding geometry*

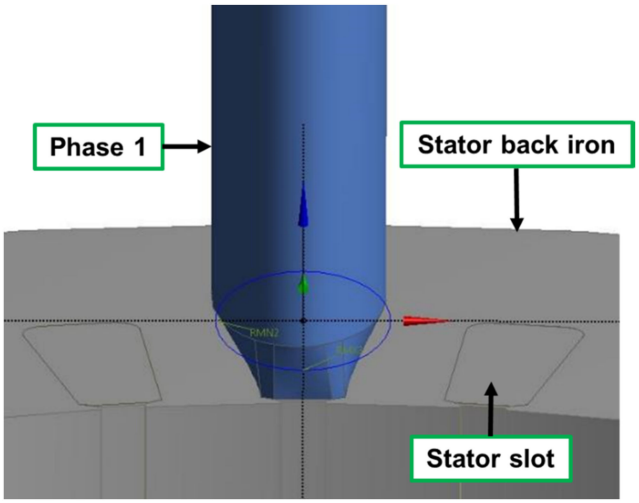

Fig. 3 *Phase 1 extrusion and change of cross section*

of analytical/empirical-based algorithms for convection boundaries. Therefore, the accuracy of this method is strongly dependent on accurate estimates of heat transfer coefficients like the LPTN approach [6].

A full thermal analysis of a TEFC machine requires a conjugate heat transfer investigation of both internal and external flows coupled with the heat sources due to electromagnetic fluxes in the rotor and stator. In this scenario, CFD is a very flexible and accurate technique thanks to its capability to provide a very detailed prediction of complex thermal and flow aspects throughout the machine to a far finer resolution compared to the LPTN approach [6]; local velocities may be calculated allowing accurate heat transfer coefficients to be obtained.

In the past, analysis has concentrated on sub-systems or components as modelling capabilities were limited by computational considerations [7–11]. However, there is now the potential to create a full system model [12], this often requires that geometrical simplifications are made and the impact that these simplifications can have on the fidelity of the answer is the subject of this paper.

Typically for TEFC machines of length and size comparable to the one under investigation, some of the most critical temperatures occur in the end windings, this paper will, therefore, concentrate on the impact geometric simplification has on the nature of the airflow in the end region area and the rate of heat transfer from the end windings.

The complexity of the end winding geometries, often consisting of several insulated copper strands bound together, provides a challenge on the modelling and analysis of heat transfer and fluid flow phenomena occurring in the end region. A number of papers have been published dealing with CFD fluid and thermal investigations in the end region of electric machines, where it is well recognised that the end region is one of the most difficulties to thermally investigate due to the complex airflow patterns [5, 13]. This complexity results in approximated and simplified geometries usually being employed to model the end windings in order to reduce the complexity of the model and the computational cost [12, 14–17].

This paper presents methodology for a more realistic end windings representation, explaining the challenges and the impact that these have on the predictions for the end region of TEFC machines.

2 CFD methodology

The motor under investigation has a distributed end windings configuration with variable pitch factor; initially, a simplified geometry, similar to those typically used, was considered as shown in Fig. 2.

Typically when using simplified geometries, some specific features from the real end winding geometry are not considered:

- Cavities between windings leaving the stator slots are neglected.
- Cavities in between the conductors are neglected.
- Conductors are not individually modelled.
- Surface roughness given by the insulated copper strands bound together is neglected: the simplified model has a totally smooth surface.

Taking into account these features of the end windings would lead to a more complex geometry and to an additional modelling effort; however, this would also provide a far more accurate representation of the whole end region of the machine.

The cavities around the end winding geometry would introduce additional fluid flow paths which would affect the prediction of the heat transfer coefficient in this region. Moreover, since in TEFC machines the internal parts are totally isolated from the surrounding external air, all the heat generated due to rotor core and stator windings losses is dissipated through the machine's outer housing. Therefore, it is very important to have, as much as possible, an accurate end winding geometry which would allow a better and accurate prediction of the complex fluid flow and thermal phenomena occurring in the end regions.

In the case under investigation, a new methodology has been developed to create a more realistic 3D end winding representation using Ansys DesignModeler, based on the individual modelling of each electrical phase with thickness and height comparable to the real geometry. Each machine's phase was extruded from the stator slots and its cross-section was turned to elliptical in order to model the roundish shape of the conductors as shown in Fig. 3.

The same approach was used to create the remaining two phases with two main differences:

- Phases 2 and 3 extrusion from the stator slot are slightly bent backwards in the radial direction in order to obtain a more roundish surface in the back of the end winding geometry.
- Phases 2 and 3 are shorter in the axial direction than phase 1 in order to model the several cavities between the conductors.

Fig. 4 reports the generated three phases; a repeating pattern was then performed for all the other stator slots in accordance to the topology of the real end winding geometry.

As a final step, a cylindrical and conical filler was introduced around the new geometry in order to model the different conductor's layers in the radial direction. Fig. 5 shows the new developed end winding geometry.

As reported in Fig. 5, the result is a new quarter symmetry end windings model with the following characteristics:

- Dimensions comparable with the real geometry.
- Several cavities between the conductors created.
- Conductor's bunch modelled in order to better represent the irregular surface as a result of the winding process.

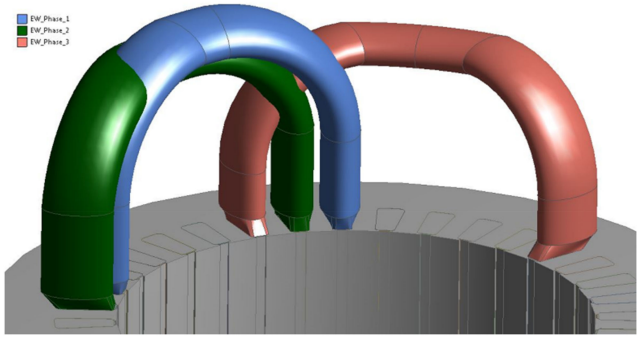

Fig. 4 *Machine's three phases*

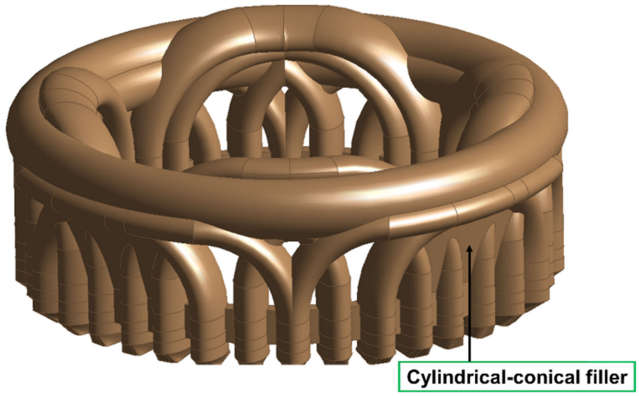

Fig. 5 *New model of more realistic end winding geometry*

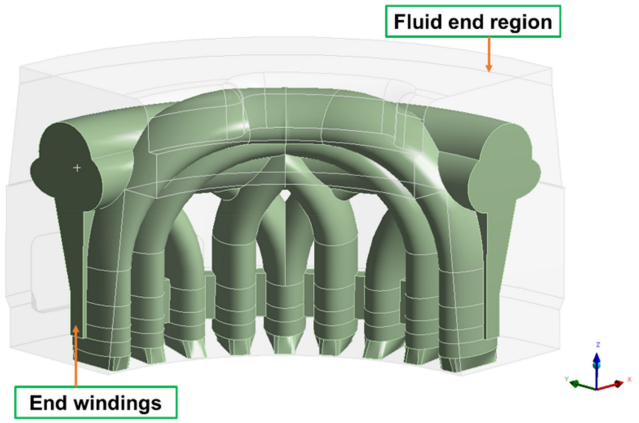

Fig. 6 *Fluid end region, 90° sector*

CFD was then utilised to investigate the flow fields present in the end region area both for the case with the simplified and the new more realistic geometry. The CFD code used in this project is Ansys Fluent, version 17.2 [18]; this solves the governing conservation equations of mass, momentum, and energy using the finite volume method.

A 3D model of the fluid end region using both the simplified and more realistic end winding geometry have been created using Ansys DesignModeler. Considering the symmetry of the machine, a 90° sector was periodically modelled as shown in Fig. 6 for the second case with more realistic geometry.

The multiple reference frame (MRF) or frozen rotor approach was used in order to simulate the rotation of the rotor around the z-axis [18]. The fluid region is split into two reference frames: one containing all rotating parts, such as the shaft, end ring, and wafters, and another stationary reference frame which contains the motor housing and the end windings; in the case under investigation, the rotational speed is set at 1500 rpm.

The realisable k-ε turbulence model was implemented since it is more suitable for rotation and high shear stresses problems and it can generally provide better performance than the standard $k - \varepsilon$ model [14].

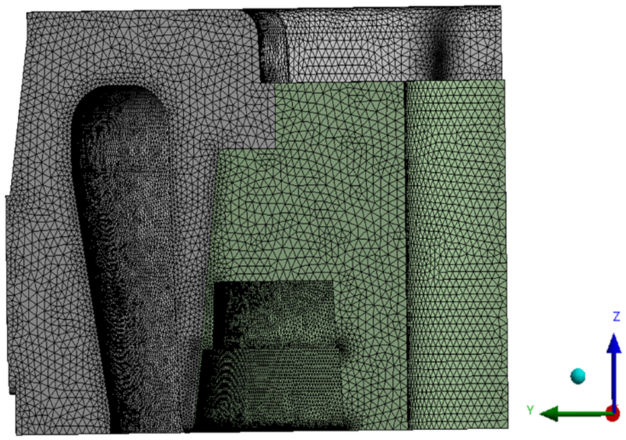

Fig. 7 *Fluid end region mesh, simplified EWs model*

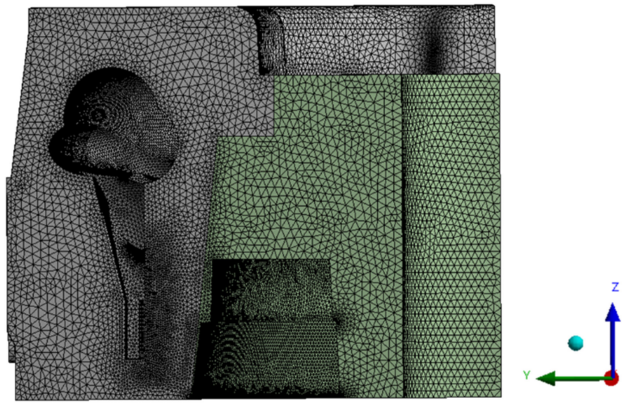

Fig. 8 *Fluid end region mesh, new EWs model*

A thermal analysis focused on convection has been conducted. Radiation has been assumed to be negligible for this application; nevertheless, all the thermal aspects and a full thermal modelling of the machine will be the object of future work.

In order to compare the convective heat transfer and heat flux dissipated through the external frame for both cases, the same physical scenario was used with appropriate thermal boundary conditions for the end windings and the housing used: the end windings and end ring walls were set at a constant temperature of 150°C, while the housing temperature was set at 100°C.

The fluid is air which is assumed to be incompressible with thermal properties, such as thermal conductivity k (W/mK) and specific heat c_p (J/kgK), set from the internal database within Ansys Fluent.

For the discretisation process unstructured meshes, with an average cell size of 2 mm, were generated within Ansys Mesher for the cases under investigation; the nature of the tetrahedral grid structure allows the new end windings geometry to be modelled without any further simplifications. According to the published literature [19, 20], a strong recirculating toroidal vortex flow, superimposed on the main swirling flow, was expected over the wafters and end windings area; therefore, in order to correctly model and capture these phenomena, local mesh refinements of 1 mm were performed in proximity of wafters and end windings surfaces. Figs. 7 and 8 shows the generated meshes for the 90° sectors of the fluid end regions using both end winding geometries.

The final meshes counted 2,075,758 and 2,490,677 cells for the case with the simplified and more realistic end winding geometry, respectively. A mesh independence study was carried out to choose an appropriate size for a good quality grid; a skewness level below 0.95 and an aspect ratio of 15 were achieved in both cases.

The PC running the simulations is a 3.70 GHz Intel Xeon Quad core CPU with 64 GB RAM running the Windows 7 64-bit operating system. A converged steady-state solution is run around 6 h for the simplified geometry case and around 9 h for the case

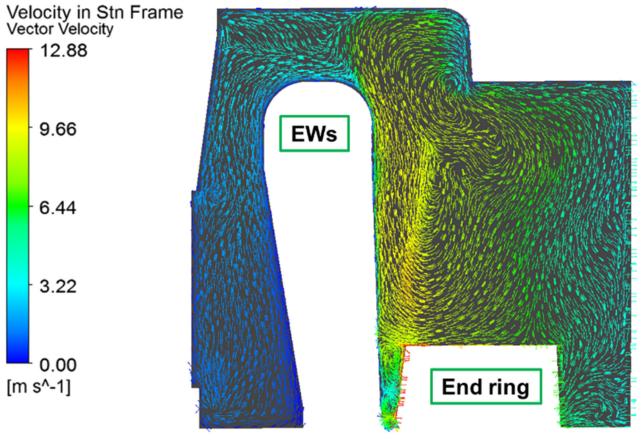

Fig. 9 *Secondary flow, simplified EWs model*

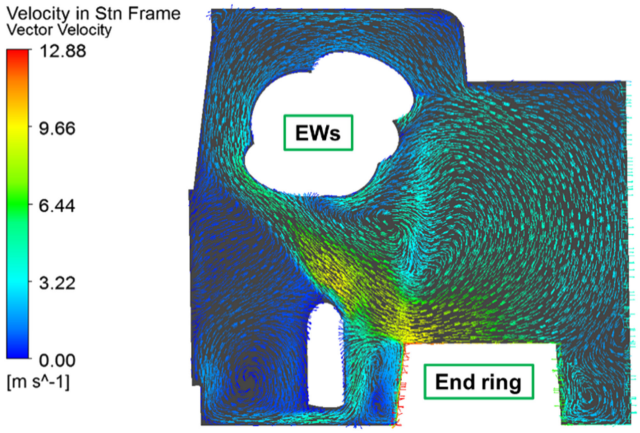

Fig. 10 *Secondary flow, new EWs model*

with the new geometry; standard residual plots of mass, velocities, turbulence quantities, energy, monitors of local velocity, and torque were used to assess convergence.

3 Results and discussions

Results compare the airflow and heat transfer in both the simplified and new end winding geometry. Figs. 9 and 10 show the secondary airflow, superimposed over the main swirling flow, plotted on an axial plane of the end ring and end windings; the axial plane location was chosen in order to better show the impact of the new end winding model's cavities on the secondary airflow of the end region.

As expected, the nature of the airflow field is similar in both cases: there is a strong toroidal vortex flow located in the region between the end windings and the end ring, while a recirculating flow, weaker in magnitude, is located in the area between the end windings and the outer frame. However, as reported in Fig. 10, the new end windings model provides a more realistic representation of the fluid flow distribution in the end region due to the higher porosity of the new geometry. In addition to the strong recirculating toroidal vortex over the end ring, the weaker recirculating flow penetrates the end windings near their base, flows upwards behind the end winding, and passes over the tip of the end winding to combine with the other main recirculating flow. The thermal behaviour of the end region is affected by the new fluid flow distribution reported in Fig. 10: a stronger convective phenomena over the end windings surface is expected where the secondary flow is stronger in magnitude and also the more uniform flow distribution through the conductor's cavities would also strongly affect the heat dissipation through the external housing. In order to investigate the thermal impact of the new end winding geometry in the end region, the heat flux (in W/m^2) dissipated through the external housing was computed as reported in Figs. 11 and 12; from the comparison with the model with the simplified end winding geometry (Fig. 11), results show how a more detailed

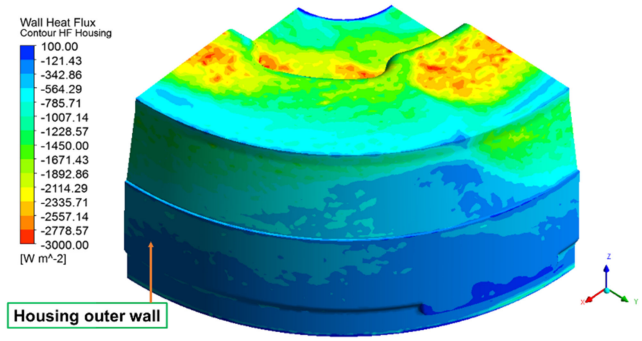

Fig. 11 *Housing wall's heat flux, simplified EWs model*

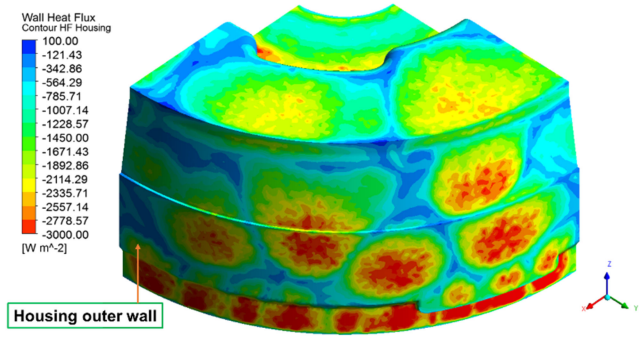

Fig. 12 *Housing wall's heat flux, new EWs model*

Table 1 Heat flow comparison, simplified and new end windings model

	Simplified EWs model [W]	New EWs model [W]	Percentage difference [%]
outer housing	31.06	49.42	45.63
end windings	17.71	33.72	62.26

end windings modelling (Fig. 12) can significantly affect the predictions of the complex thermal phenomena occurring in the end region; the heat dissipation rate through the outer housing increases by up to 45%.

Table 1 reports the comparison between the CFD results of heat flow [W] for outer housing and end windings for the cases under investigation; the percentage difference was calculated as shown in (1).

$$\%\text{diff} = \frac{\left|\text{Heatflux}_{(\text{simpl. model})} - \text{Heat flux}_{(\text{new model})}\right|}{\frac{1}{2}\left(\text{Heatflux}_{(\text{simpl. model})} + \text{Heat flux}_{(\text{new model})}\right)} \times 100 \quad (1)$$

4 Conclusion

Since in TEFC machines the internal parts are totally isolated from the surrounding external air, all the heat generated due to rotor core and stator windings losses is dissipated through the machine's outer housing; therefore, it is very important to have, as much as possible, an accurate end windings representation which would allow a more realistic prediction of the complex fluid flow and thermal phenomena occurring in the end regions.

Here, a new modelling approach for a more realistic end windings representation, which potentially can be applied also to different kind of machines, has been developed and presented; the new geometry has comparable topology and dimensions with the real end winding geometry of the motor under investigation.

A CFD fluid and thermal analysis of the end region area was carried out in order to investigate the impact of the developed geometry on the airflow distribution and on the rate of heat transfer from the end windings to the external housing. Results from the comparison with a simplified end winding geometry show how a more accurate and detailed representation can significantly affect

the prediction of the complex thermal phenomena occurring in the end region; in particular, the heat dissipation rate from the end windings and through the outer housing increase up to 62.26% and 45.6%, respectively.

Experimental validation will be object of future work: internally placed thermocouples are going to provide thermal measurements of stator, end windings and end region's air to be used to validate the CFD model. Moreover, a CFD conjugate analysis of the full TEFC machine, modelling both external and internal flows and solid parts, is already in progress in order to deeply investigate the impact of the new developed end winding geometry on the full CFD machine model.

5 Acknowledgments

The financial support from *ABB Corporate Research* for this research is gratefully acknowledged.

6 References

[1] Pyrhonen, J., Jokinen, T., Hrabovcová, V.: '*Design of rotating electrical machines*' (Wiley, Chichester, West Sussex, United Kingdom, 2014)

[2] Staton, D., Boglietti, A., Cavagnino, A.: 'Solving the more difficult aspects of electric motor thermal analysis in small and medium size industrial induction motors', *IEEE Trans. Energy Convers.*, 2005, **20**, (3), pp. 620–628

[3] ABB Group, Low voltage motors Motor guide

[4] Valenzuela, M.A., Tapia, J.A.: 'Heat transfer and thermal design of finned frames for TEFC variable speed motors'. IEEE Industrial Electronics, IECON 2006–32nd Annual Conf., Paris, France, November 2006

[5] Micallef, C.: 'End Winding Cooling in Electrical Machines'. PhD thesis, University of Nottingham, 2006

[6] Boglietti, A., Cavagnino, A., Staton, D.*, et al.*: 'Evolution and modern approaches for thermal analysis of electrical machines', *IEEE Trans. Ind. Electron.*, 2009, **56**, (3), pp. 871–882

[7] Mugglestone, J., Pickering, S.J., Lampard, D.: 'Effect of geometric changes on the flow and heat transfer in the end region of a TEFC induction motor'. Ninth Int. Cinference on Electrical Machines and Drivers (Conf. Publication no 468), Canterbury, UK, 1999

[8] Micallef, C., Pickering, S.J., Simmons, K.*, et al.*: 'Improvements in Air flow in the End region of a large totally enclosed Fan cooled induction motor'. IEEE Int. Conf. on Electric Machines and Drives, San Antonio, USA, 2005

[9] Hettegger, M., Reinbacher-Kostinger, A., Biro, O.: 'Characterizing the convective wall heat transfer on convoluted shapes in the end-region of an induction machine'. 2012 XXth Int. Conf. on Electrical Machines (ICEM), Marseilles, France, 2012, pp. 1219–1226

[10] Saliba, A., Micallef, C.: 'Investigating the cooling performance of the end region of a small totally enclosed Fan cooled (tefc) induction motor'. 5th IET Int. Conf. on Power Electronics, Machines and Drives (PEMD 2010), Brighton, UK, 2010, pp. 1–6

[11] Takahashi, K., Kuwahara, H., Kajiwara, K.*, et al.*: 'Airflow and thermal conductance in a totally enclosed induction motor', *Heat Transf. Asian Res.*, 2002, **31**, (1), pp. 7–20

[12] Connor, P.H., Pickering, S.J., Gerada, C.*, et al.* 'CFD modelling of an entire synchronous generator for improved thermal management'. 6th IET Int. Conf. on Power Electronics, Machines and Drives (PEMD 2012), Bristol, 2012, pp. 1–6

[13] Micallef, C., Pickering, S.J., Simmons, K.A.*, et al.*: 'Improved cooling in the end region of a strip- wound totally enclosed fan-cooled induction electric machine', *IEEE Trans. Ind. Electron.*, 2008, **55**, (10), pp. 3517–3524

[14] Xu, Z., La Rocca, A., Pickering, S.J.*, et al.*: 'Mechanical and thermal design of an aeroengine starter/generator'. IEEE Int. Electric Machines & Drives Conf., Coeur D'Alene, USA, 2015

[15] Jungreuthmayer, C., Bäuml, T., Winter, O.*, et al.*: 'A detailed heat and fluid flow analysis of an internal permanent magnet synchronous machine by means of computational fluid dynamics', *IEEE Trans. Ind. Electron.*, 2012, **59**, (12), pp. 4568–4578

[16] Kral, C., Haumer, A., Haigis, M.*, et al.*: 'Comparison of a CFD analysis and a thermal equivalent circuit model of a TEFC induction machine with measurements', *IEEE Trans. Energy Convers.*, 2009, **24**, (4), pp. 809–818

[17] La Rocca, S., Eastwick, C.N., Connor, P.*, et al.*: 'Challenges in modelling totally enclosed fan-cooled electrical machines'. Int. Heat Transfer Symp. and Heat Powered Cycles Conf., Nottingham, UK, 2016

[18] ANSYS Mesher and Fluent 17.2, User manual

[19] Oslejsek, O.: 'The cooling of the end winding of small enclosed electric machines', *Elektrotech. Obz.*, 1972, **61**, (10), pp. 548–556

[20] Mugglestone, J., Pickering, S.J., Lampard, D.: 'Prediction of the heat transfer from the end winding of a TEFC strip-wound induction motor'. Proc. IEEE IEMDC, Seattle, WA, May 1999, pp. 484–486